Effectiveness of hybrid powertrains to reduce the fuel consumption and NOx emissions of a Euro 6d-temp diesel engine under real-life driving conditions

José Manuel Luján, Antonio García, Javier Monsalve-Serrano* and Santiago Martínez-Boggio

CMT - Motores Térmicos, Universitat Politècnica de València, Camino de Vera s/n, 46022 Valencia, Spain

Energy Conversion and Management, Volume 199, 1 Nov 2019, 111987

https://doi.org/10.1016/j.enconman.2019.111987

Corresponding author (*):
Dr. Javier Monsalve-Serrano (jamonse1@mot.upv.es)
Phone: +34 963876559
Fax: +34 963876559

Abstract

Recent investigations demonstrated that the real-world driving conditions differ from those proposed in the homologation cycles. This provokes that the emissions levels in real-life conditions exceed the normative values, as shown in the recent scandal related to the NOx emissions from the passenger cars equipped with diesel engines. On the other hand, the upcoming emissions regulations will limit the CO_2 emissions to very low levels, which demands a further optimization of the existing technology. One way to reduce the NOx and CO_2 emissions is by electrifying the powertrain in a certain degree. The objective of this work is to evaluate the potential of implementing a parallel (P2) hybrid architecture in a compact car (class C) equipped with a diesel 1.6 Euro 6d- temp engine to reduce the emissions and fuel consumption in homologation and real-life driving cycles. This has been done using a 0D numerical vehicle model and the experimental engine maps of fuel consumption and emissions measured at steady state conditions. After that, the transient conditions were simulated in homologation cycles and real-life driving cycles measured by the authors in Spain. The numerical model was validated against experimental tests carried out in an active engine test bench, evidencing differences below 4% under the worldwide harmonized light vehicles test cycle (WLTC). In the real-life cycles, the hybridization of the powertrains improves the fuel consumption for all types of driving cycles (urban, combined and highway). The major benefits are obtained in urban driving cycles, with gains up to 50% in fuel consumption and CO_2 emissions. In addition, the improvements in real-life conditions are higher than in the urban phase of the homologation cycles. On the contrary, combined real-life cycles (urban + rural + highway) show lower benefits than the homologation cycle. This is due to different energy management strategy that needs to be adapted to each driving situation. Lastly, it was found that, contrarily to the case of the homologation cycle, the NOx emissions are not reduced with the hybridization of the diesel powertrain in real-life conditions. Thus, to achieve 2021 CO_2 target (95 g/km) and to reduce aftertreatment systems in diesel engines, other vehicles technologies need to be added to the full hybridization.

Keywords

Hybrid powertrain; Diesel Internal Combustion Engines; Emissions regulations; Driving cycles

1. Introduction

Pollutant emissions regulations have become more and more stringent in the recent years, especially for conventional diesel combustion (CDC) engines [1]. Manufacturers were forced to incorporate complex aftertreatments systems, as diesel particulate filter (DPF) and selective catalyst reduction (SCR), to achieve the required soot and NOx targets (0.05 g/km and 0.08 g/km, respectively, for Euro 6). However, these aftertreatment elements increase the total cost of the vehicle, reduce the engine efficiency and are not allow to reduce greenhouse emissions [2]. Carbon dioxide (CO_2) emissions are gaining all the attention in the transportation sector due to the high increase of the global temperature in the last years. Passenger cars produce around 20% of the total emissions of CO_2 in the European Union (EU) [3]. Therefore, representatives of the European Commission, Parliament, and Council agreed on a compromise to add limitations in CO_2 in the present emission regulation. The agreed-upon targets aim to reduce the average CO_2 emissions from new cars by 15% in 2025 and by 37.5% in 2030, both relative to a 2021 baseline (95 gCO_2/km) [4]. As it is well known, the CO_2 emissions mainly depends on the fuel carbon content and fuel consumption. Therefore, it is necessary to keep pushing to find new advancement for the reduction of emissions and cost. Several authors affirm that more efficiently powertrains and e-fuels are potential ways to achieve the desired targets [5,6].

In order to improve the current powertrains, hybrid architectures combining electrical components and high-efficient internal combustion engines (ICE) were demonstrated to be a reliable solution that can be applied in a short term perspective [7]. A hybrid electric vehicle (HEV) is defined as a combination of an ICE and one or various electric motors (EM) connected to powerful battery package [8]. It is an intermediate solution between the current conventional powertrains and pure electric vehicles (EVs). The application of EVs has encountered shortcomings, such as long battery charging time, limited operating range and not clear improvements in the well-to-wheel (WTW) and life cycle CO_2 emissions [9]. The not renewable electric sources [10,11] and high CO_2 emissions in production and recycling of electric components [11] are the main reasons to this not clear scenario. In terms of hybrid vehicle categories, a first classification is done depending on the battery capacity and the charge source (internal or electricity grid): mild (MHEV, <60v, <2kWh, not external electric connection), full (FHEV, >60v, <15kWh, not external electric connection) and plug-in (PHEV, >60v, >15kWh, external electric connection) electric vehicles [12]. Another category depending on the powertrain architectures as: belt alternator assists (P0), parallel (P2), series and series-parallel (or power split). The main difference is found in the setup of the electric motor(s) with respect to the ICE. Based on different topological complexities and costs of these types of HEVs, the parallel full hybrid configuration shows potential due to the possibility to avoid large modifications with respect to the OEM, be independent from the electric grid and provide savings around 15-25% with respect to the homologous conventional powertrain [8,13,14]. In general, the information available about fuel consumption and emissions during the vehicle marketing is based on the homologation cycle. However, it is well known that depending on the real use of the vehicle, these values can differ substantially [15,16].

The current homologation procedure, worldwide harmonized light-duty vehicles test procedures (WLTP) [17], was created taking around 765.000 km of real-world driving data from five regions (Europe, India, Japan, Korea and USA) [17]. The aim was to overcome the great difference that existed from the old procedure (new European driving cycle, NEDC) and real-life driving cycles. The WLTP has two parts, one that is performed in a chassis dynamometer using a standard driving cycle (the worldwide harmonized light vehicles test cycle, WLTC) under controlled laboratory conditions. The second part of the WLTC entails testing the vehicle in a real driving emissions (RDE) test, in which the vehicle pollutant emissions are measured in the road by using portable emissions measurement systems (PEMS) [18]. A previous work of the research group [1] shows that under RDE conditions, the number of accelerations during the urban phase and the test time are substantially higher than in a NEDC or WLTC. Moreover, it was found that, for a conventional powertrain, the highest portion of NOx are emitted at low speeds with zones of more accelerations and decelerations, characteristics of urban areas. Several works in literature have compared the fuel economy and emissions of conventional powertrains equipped with spark ignition (SI) engines [19,20] and diesel engines [21,22] under different driving cycles [15]. These works demonstrate that compression ignition (CI) engines are the optimal choice in terms of efficiency, providing lower CO_2 emissions than SI engines at the same test condition [23,24]. In spite of the high efficiency of CI engines, future regulations will impose drastic reductions of the CO_2 emissions. In order to successfully master the upcoming legislative challenges, further increased electrification/hybridization of the vehicle powertrain is crucial. Hybridization has been shown to be an effective way to reduce the CO_2 from spark ignition engines [25]. However, there are limited number of works that have confirmed this advantage in hybrid diesel platforms. Huo et al. [26] studied the improvements of different control strategies in the FTP75 in a parallel hybrid vehicle. They found that use of optimal control models allows a reduction of 5% with respect to traditional rule-based control (RBC) strategies. The study carried out by Gupta et al. [13] analyzes the potential of a light duty diesel pickup with hybrid technology in the modified Indian driving cycle (MIDC). The hybrid vehicle is about 30% faster than the equivalent conventional vehicle. Fuel economy is improved in the order of 26%. Up to the knowledge of the authors, there are no scientific works studying the diesel-hybrid vehicle concept in the present WLTP legislation and in real-life cycles.

Therefore, the aim of this manuscript is to study the potential of a diesel parallel (P2) hybrid powertrain in several real-life driving conditions. The different components of the hybrid vehicle platform were optimized to achieve the minimum possible fuel consumption and NOx emission in the actual WLTP legislation. To do this, numerical vehicle simulations for conventional and hybrid powertrain were performed. The numerical model was validated through experimental tests in Euro 6d-temp diesel engine representative of a C-segment passenger car. The hybrid powertrain was controlled by means of an in-house developed rule-based control power management strategy. Finally, an overall vehicle energy analysis was performed to compare the optimum hybrid platform versus the conventional powertrain from the original equipment manufacturer (OEM).

2. Materials and methods

2.1. Engine and test cell

The experiments were performed on a dynamic test bench with a turbo-charged diesel engine, which is Euro 6d-temp compliant. Table 1 shows the main features of the engine. The engine includes both low pressure and high pressure EGR systems. Also, it has a variable geometry turbocharger (VGT) that allows to change the load of the intake pressure by changing the blades position. The original equipment manufacturer system and engine calibration was used to study the potential of actual diesel engines in a hybrid powertrain.

Table 1 – Engine Specifications

Cylinder number	4 in-line
Bore	80 mm
Stroke	79.5
Displacement	1600
Compression ratio	15.4:1
Valve number per cylinder	4
Fuel/System	Diesel/Common rail direct injection
EGR system	High and low pressure cooled
Intake Boosting	Turbocharger with VGT
Maximum Power	96 kW @4000 rpm
Maximum Torque	320 Nm @ 1750 rpm

The experimental test was performed in a dynamic test bench with a Horiba Dynas3 LI250 (Figure 1) that allows to work in stationary and transient conditions by imposing the required engine speed and torque. The first step of this work was to perform the measurements of 54 stationary points at different engine speeds (850 rpm to 2850 rpm) and 7 load levels (brake torque from 10 Nm to 250 Nm). This allows to build the engine calibration maps by means of a linear interpolation. Therefore, it is possible to determine the brake specific fuel consumption (BSFC), and brake specific emissions ($BSNO_x$ and $BSCO_2$) for any operative condition required in a transient cycle. These maps are the main input for the numerical model that it is used to study the vehicle operation under different driving cycles. As second step, the driving cycles selected are simulated by means of the GT-Drive model for conventional and hybrid powertrains. The required engine speed and torque are obtained as output of the numerical model and inserted into the experimental test bench software control. Therefore, thanks to the capabilities of the active dynamometer, the fuel consumption and emissions are measured in different driving cycles in the real engine test bench and compared to the results obtained in the simulations.

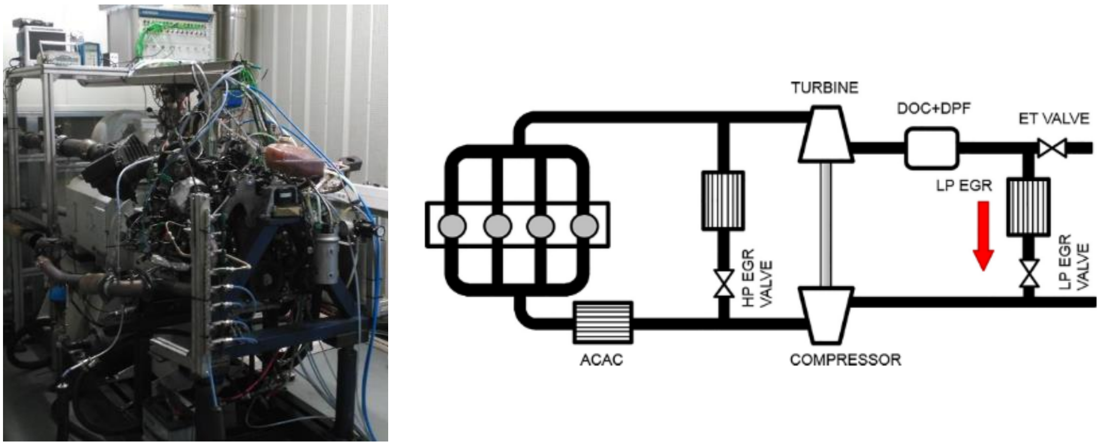

(a) (b)

Figure 1 – Dynamic engine test cell and instrumentation devices (a) and diesel engine air management scheme (b).

The instantaneous fuel consumption was measured with an AVL gravimetric fuel balance and the exhaust gas composition was measured with a Horiba MEXA 7170DEGR, which acquires the engine-out NOx, THC, CO, CO_2, and O_2 concentrations (before the aftertreatment systems). The EGR rate has been obtained experimentally from the CO_2 measurement in the exhaust and intake manifolds. The instrumentation characteristics are presented in Table 2.

Table 2 – Test bench sensor characteristics and capabilities.

Variable	Sensor	Accuracy	Range
Engine Torque	Dynamometer brake	0.1%	0-480 Nm
Temperature at intake, exhaust, cooling water and lubricant circuit	Thermocouple	1.0%	0-1260 ºC
Pressure at intake, exhaust, cooling water and lubricant circuit	Pressure sensor	0.3%	0-6 bar
Fuel mass consumption flow	Gravimetric fuel balance	0.2%	0-150 kg/h
Intake mass flow	Hot wire meter	1.0%	0-720 kg/h
Engine exhaust Emissions	HORIBA MEXA-170DEGR	3.0%	----

2.2. Vehicle, numerical model description and validation

2.2.1. Vehicle

The engine used in this work is originally used in a C-segment car (Nissan Pulsar C13) which is sold since 2016 in Japan, Europe and China among others. It is important to note that in Europe the 88% of light-duty engines are used for passengers transportation, with 49% working with diesel as fuel source [28]. In addition, only 2.5% of the cars are hybrid (FHEV or PHEV) and 0.4% full electric. Therefore, to insert new technologies with a combination of traditional powertrains with electric components still represents a big challenge in the automotive industry. In terms of vehicle power, the average value in Europe is around 95 kW, with Germany being over the average (110 kW) and France being below (80 kW). This is because the compact vehicles cover more than the 30% of the European market. Similar statistics are seen in other regions as Asia and South America. Therefore, the vehicle selected in this work (C-class, Diesel, 96 kW and conventional powertrain) is representative of large part of the vehicles used around the world.

The main vehicle characteristics are shown in Figure 2. The diesel Euro 6d-temp engine is coupled in a traditional powertrain. This means that the vehicle is propelled only by the thermal engine, and the engine speed is converted by a manual six gears transmission with the following ratios: 13.9, 7.4, 4.8, 3.2, 2.4 and 2.1 including the differential ratio.

Parameter	Value
Class	C-segment
Vehicle Total Weight	1581 kg
Front Area	2.8 m^2
Drag Coef.	0.3
Wheels	205x50 R17
Rolling Friction Coef.	0.013
Transmission	6-manual

Figure 2 – Vehicle Specifications.

As was mentioned in the previous section, a numerical 1D model was used to simulate the behavior of the all powertrain. The commercial software GT-Suite of Gamma Technologies® (v2018, Gamma Technologies, LLC., Westmont, IL, USA, 2018) was used due to the capabilities of simulate the entire vehicle with models for gearbox, tires, axles and couplings, etc. In addition, the software also has the necessary devices to perform the hybridization process, which results in different electric motors, batteries and controllers. The driving cycle (time vs vehicle speed and altitude vs distance) is inserted in the driver module who controls the accelerator position, brake pedal position, transmission gear number and clutch pedal position. This component allows the control of the vehicles with manual transmissions as it contains the necessary functions for the vehicle launch and shifting. The model consists of a feed forward component which calculates the engine load torque (or wheel braking torque) required for a targeted vehicle speed or acceleration. Once the reference load torque is calculated, a standard PID controller is used to correct the demanded load from the engine or brakes to minimize the remaining error between the target vehicle speed and the actual speed value.

The engine maps from the stationary experimental tests were used as inputs for the simulation in the engine module. This object describes the attributes of the internal combustion engine through a map-based engine model that describes the engine performance (power output and friction), fuel consumption, heat rejection and emissions, among others. Therefore, each operating condition required to perform the driving cycle is simulated as a different point of the engine map. This approach has been used in the past by several authors since it allows to describe a transient phenomenon from an initial study in stationary conditions with an error for the fuel consumption and emissions generally below 5% and 10%, respectively [29,30].

2.2.2. Numerical Model description

In this study, two different powertrains are simulated. The first one is the OEM configuration, which is a conventional powertrain representative of most part of the current commercial vehicle. The second powertrain is a parallel pre-transmission (also called P2) full hybrid vehicle (FHEV). The latter architecture is already used by several companies as Honda (Civic), Hyundai (Sonata and Ionic) and Mercedes (S400) among others. It has an electric motor (EM) coupled with the ICE and the transmission by two different clutches that allows to work separately or together depending on the powertrain state. In addition, it is possible to recharge the battery and recover the energy when the car is braking. The transmission is followed by a differential and coupled to the front wheels. A complete layout of the powertrains is depicted in Figure 3. The main advantage of this technology is the requirement of only one EM (traction/generator) and the possibility of using already well-developed components as the transmission and clutches, among others.

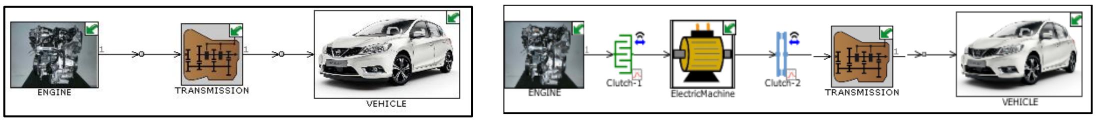

(a) (b)

Figure 3 - Powertrain layout for conventional powertrain (OEM) (a) and parallel full hybrid electric vehicle (P2 FHEV) powertrain (b).

The control system can change the hybrid powertrain state in mainly four different operation modes: 1) Pure electric mode, in which the EM propels the vehicle with the ICE off. 2) Torque Assist mode, in which the EM and ICE propel the vehicle together. 3) Range extender mode, in which the ICE propels the wheels and charge the battery with the EM being in generator mode. 4) Regenerative Braking, in which the EM absorbs the power to reduce vehicle speed. If the necessary braking torque is more than the maximum torque of the EM, the conventional friction brakes add the necessary torque to stop the car. More details of the hybrid state, changes between them and model details can be seen in a previous work of the research group [31].

2.2.3. Numerical model validation

The stationary maps of the original engine calibration were measured experimentally to be inserted as the main input of the numerical model to reproduce the transient behavior of the vehicle. Figure 4 shows the BSFC and engine-out NOx emissions values. The color scale shows an increase of the values from the blue to the red zones. The absolute values are not depicted in the maps due to confidentiality reasons, but the analysis can be performed by means of the qualitative engine maps. The maps are only depicted from 850 rpm to 2850 rpm because it is a representative engine operation range for a normal use of the vehicle during a driving cycle. From Figure 4a, it is possible to see that the engine thermal efficiency increase with the load, and the maximum efficiency is seen at high engine speeds (above 1500 rpm) and loads (above 8 bar BMEP). On the other hand, the NOx emissions are minimum at low speed and load. This is to reduce the NOx emissions in the representative area of the WLTC proposed by the Euro 6 legislation. The maximum NOx levels are seen at medium load and speed conditions. Therefore, to reduce the NOx emissions, the control system of the new hybrid powertrain needs to avoid this zone (1850 rpm and 12 bar BMEP).

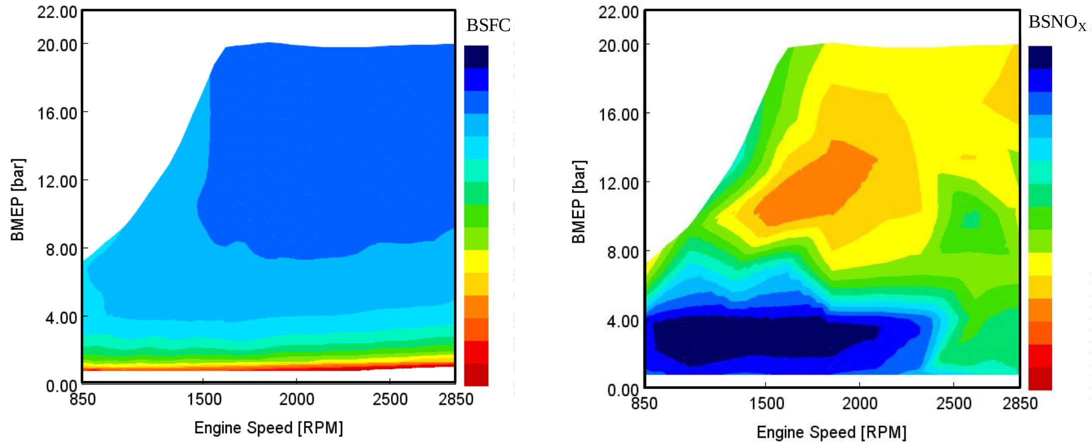

(a) (b)

Figure 4 – Engine Maps of brake specific fuel consumption (a) and brake specific NOx engine-out emissions (b) at stationary conditions.

The numerical model validation was performed to check the accuracy of the simulated values. The 1D model results were compared against the results from the driving cycle performed in the experimental test bench. The campaign is focused on validating the fuel consumption and emissions of the ICE instead of validating the behavior of the electric components or powertrain elements as transmission, vehicle forces or wheels behavior. This approach was used by several authors [32] due to the simplification and cost reduction while maintain an acceptable accuracy of the results. It is well known that the ICE is one of the most difficult components to be simulated due to the effect of the transient phenomena.

The model validation was performed in the WLTC Class 3b, which is the homologation cycle for almost all the passenger cars [33]. The ICE speed and torque required to perform the cycle was imposed in the test bench. All the test was performed in warm conditions to be comparable with the engine maps performed previously. The conventional powertrain was equal to the OEM with the suggested transmission shift strategy by the OEM. For the hybrid model, a 22 kW EM and a battery package of 400 V and 10 kWh was used. These values were used as representative of a P2 FHEV [13]. Later in this work, these values will be modified to obtain the optimum powertrain configuration.

The comparison between the experimental and simulated results for the accumulated fuel consumption and NOx emissions is reported in Figure 5. The results show that the accuracy of the model is good for both powertrains and both parameters. It is important to note that the hybrid vehicle operates under pure electric mode up to 850 seconds, after that the ICE is turned on. The instantaneous values show that the model is capable to follow the fuel consumption (Figure 6a) and NOx emissions (Figure 6b) from the experimental test. In this sense, the model presents higher NOx peaks than the experimental trace, mainly due to small differences in the transient behavior and the ICE cooling temperature. For the sake of brevity, the instantaneous values for OEM and CO_2 emissions are not shown. However, a summary of all the results is depicted in Table 3. As it can be seen, the numerical results show good agreement with the experimental data and the validation is performed with success.

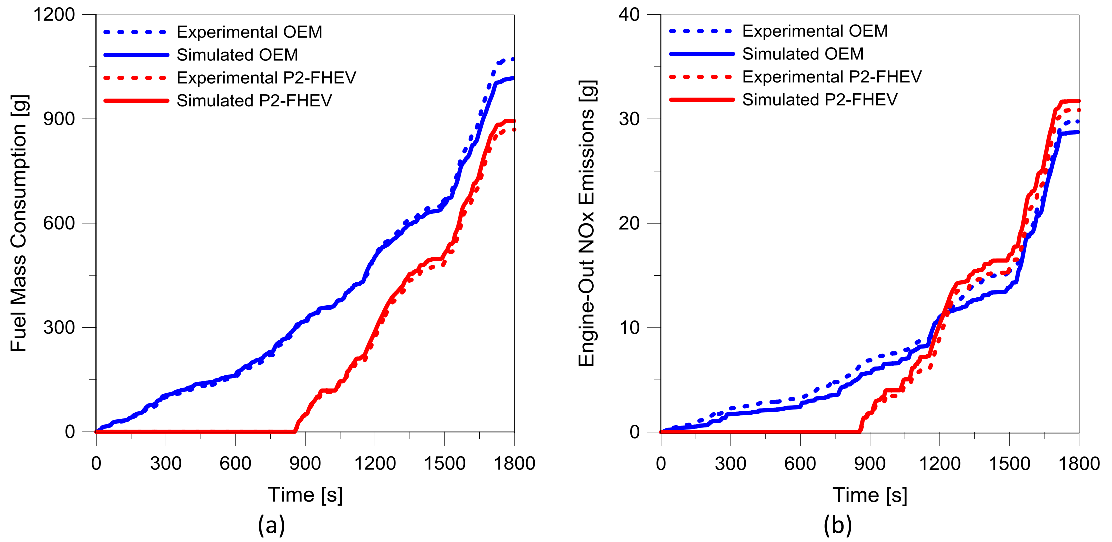

Figure 5 – Experimental against simulated fuel consumption (a) and NOx engine-out emissions (b) for OEM and P2-FHEV powertrain in the WLTC.

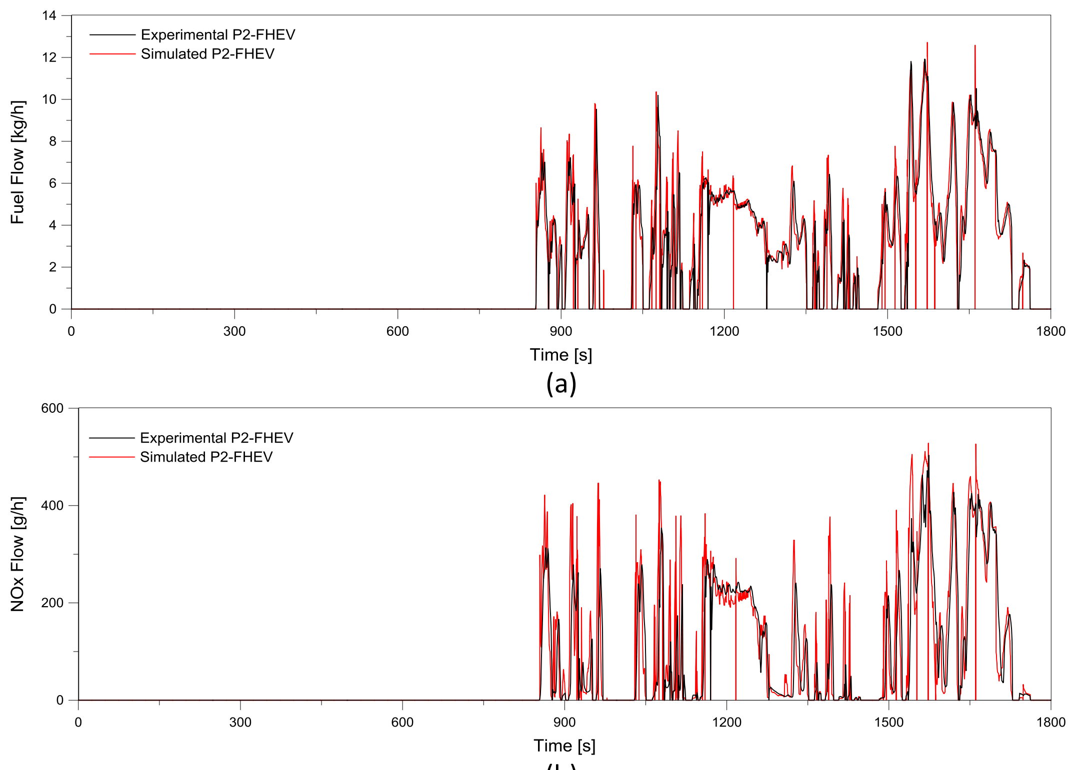

Figure 6 – Experimental against simulated instantaneous fuel consumption (a) and NOx engine-out emissions (b) for P2-FHEV in the WLTC.

Table 3 – Comparison between experimental and numerical model for the main engine outputs at WLTC.

Powertrain	Test	Fuel Consumption [g]	Dif [%]	CO_2 Emissions Engine-Out [g]	Dif [%]	NOx emissions Engine-Out [g]	Dif [%]
OEM	Experimental	1071	4.8	3125	0.2	29.8	3.4
	Simulated	1020		3120		28.7	
P2-FHEV	Experimental	869	2.8	2643	1.7	30.8	3.0
	Simulated	894		2690		31.7	

2.3. Homologation and Real-Life Driving cycles

As the aim of this work is to compare the behavior of a full hybrid parallel (P2) vehicle in real-life driving cycles against the conventional vehicle (OEM), several real driving cycles were measured and then simulated. Moreover, the cycle proposed by the current homologation procedure for conventional and hybrid passenger cars in Europe (WLTP) was used to optimize the hybrid vehicle as well as a reference for comparison.

In detail, the WLTP regulation stablishes that conventional and full hybrid vehicles need to pass the WLTC and RDE driving cycles with emissions values below the Euro 6 limits. The first one is a predefined cycle (Figure 7a) with four different zones; low, medium, high and extra-high, that represent all the conditions that can be found during a normal daily route. In the homologation procedure, this test is performed in a vehicle test bench in controlled conditions. On the other hand, to ensure the homologation procedure is representative of the real driving conditions, the normative requires passing and additional cycle called real driving emissions (RDE) cycle. For that purpose, the cycle has to meet some characteristics such as ambient, dynamic and driving conditions described in the RDE regulation [34]. A portable emissions measurement system (PEMS) is used to the measure the emissions on board. Figure 7b shows a driving cycle measured by the authors that meet RDE constrains [34] and it was used in previous work to compare conventional powertrains [1].

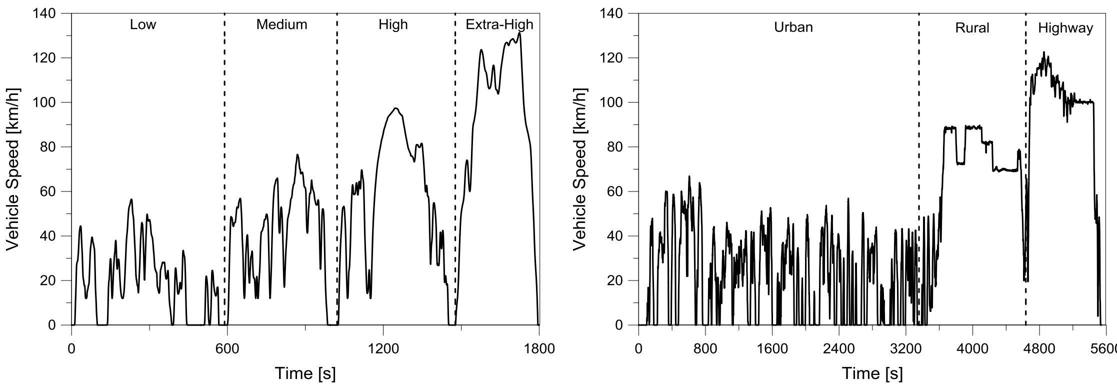

(a) (b)

Figure 7 – Homologation cycles under the new WLTP legislation for light duty vehicles. WLTC (a) and RDE (b) driving cycles.

Apart from the WLTC and RDE, the vehicle-speed profiles of several real-life routes were measured in order to study the differences versus the homologation cycles. In detail, measurements of latitude, longitude and elevation were performed with a GPS data logger and then processed to obtain time versus speed traces and elevation versus distance data. The routes were performed in the region of Valencia and Madrid (Spain) with a passenger car (no-hybrid). In the postprocessing, the different routes are divided in urban cycles and combined cycles, as done in the normative. An urban cycle is generally performed in the city center with vehicle speeds below 60 km/h. Rural areas correspond to zones with vehicle speeds between 60 to 90 km/h and correspond to the transition between the city and the highway. This last driving zone has speeds above 90 km/h, with a top speed around 120-140 km/h and distance longer than 100km. The mentioned cycles are depicted in Figure 8, Figure 9 and Figure 10, respectively.

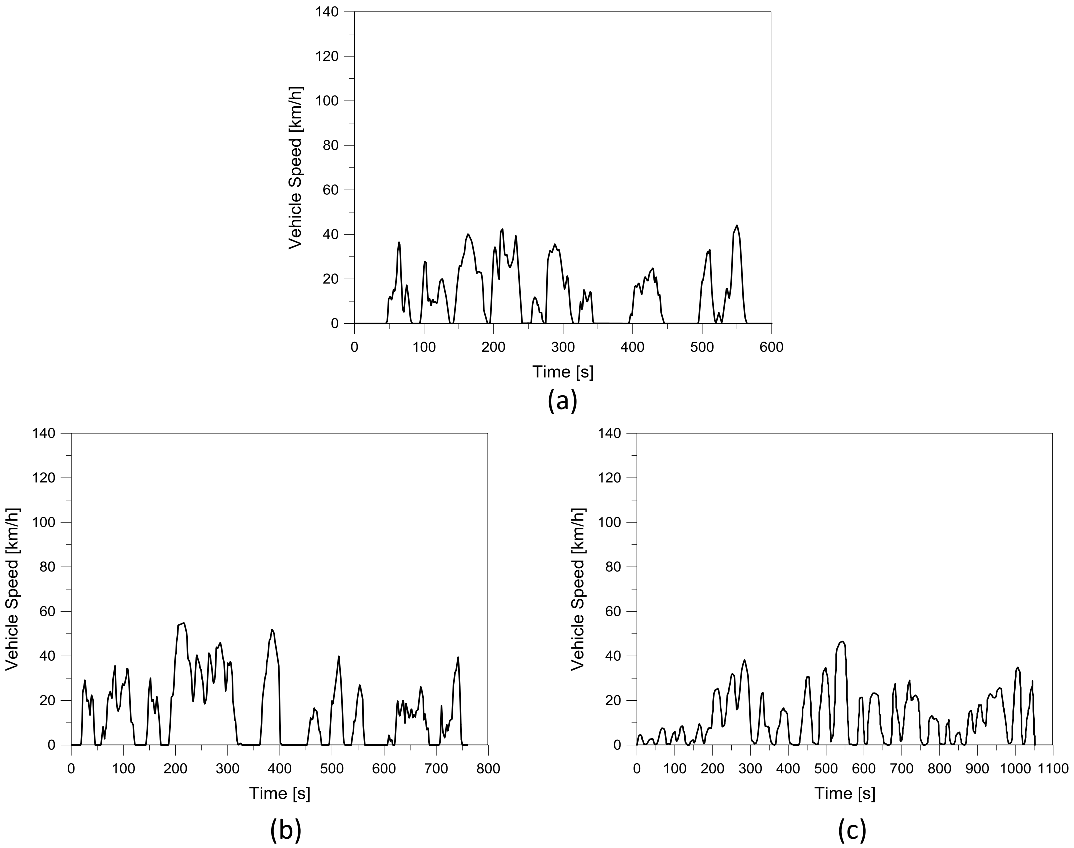

Figure 8 – Real-life driving cycle in urban areas.

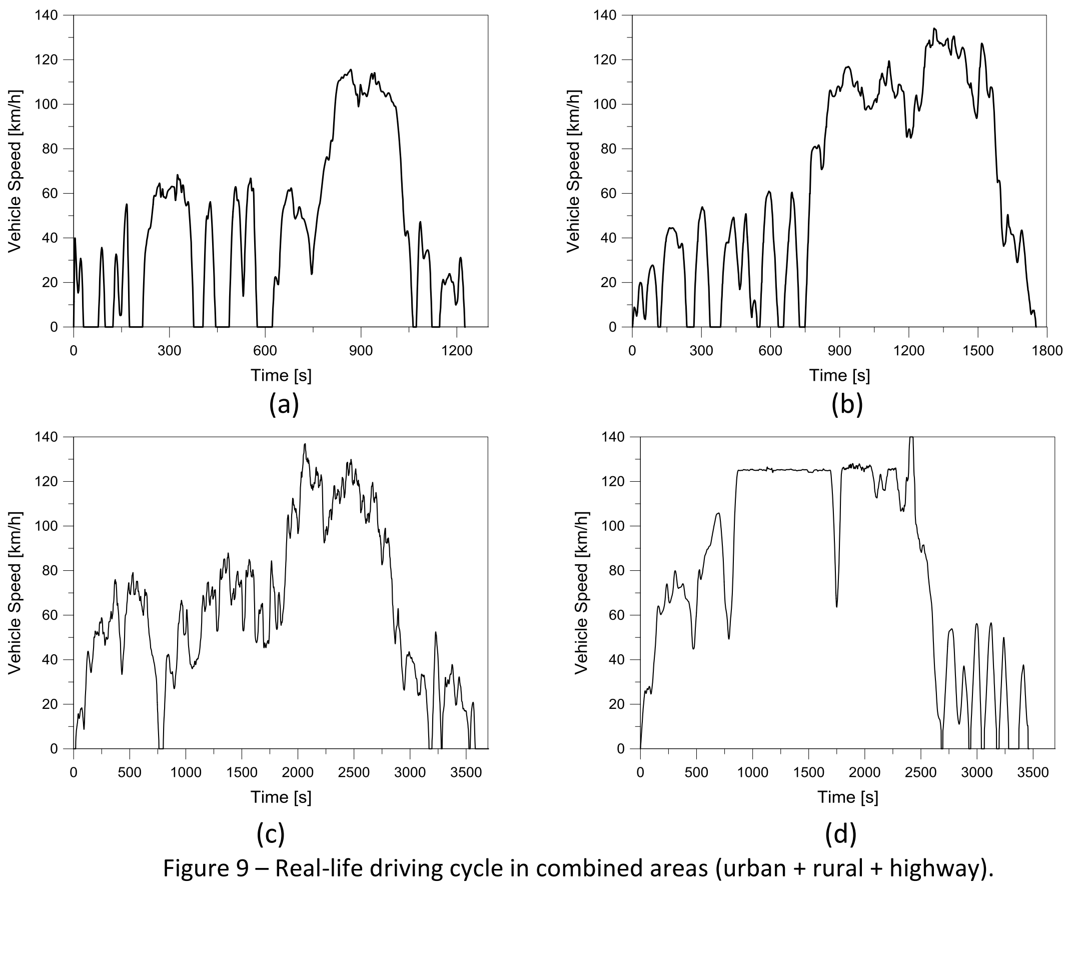

Figure 9 – Real-life driving cycle in combined areas (urban + rural + highway).

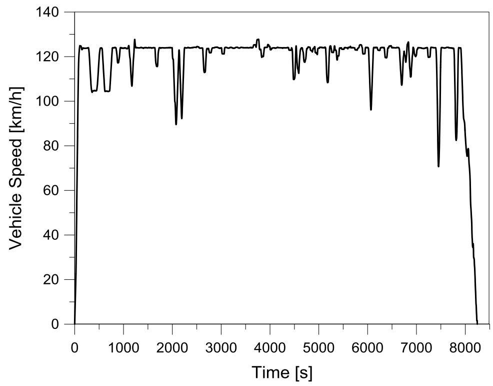

Figure 10 – Real-life driving cycle in highway.

A summary of the main characteristics of the cycles is shown in Table 4. The maximum speed is reached at combined 4 (20 km/h over the legal limit in Spain). However, it was included because represents a possible scenario of real-life cycles. Urban cycles were below 55 km/h in all cases and the accelerating, deaccelerating and standing times were closer (around 30%). The combined real-life cycles show a higher balance between accelerations and deaccelerations than the homologation cycle, and in most of the cases the standing time was lower. The highway cycle represents a typical long trip (>200 km) that is practically performed at 120 km/h cruise speed. Each of these characteristics are important for the well understanding of the results obtained.

Table 4 – Main characteristics of the driving cycle tested.

Driving cycle	Distance [km]	Time [s]	Max Speed [km/h]	Max altitude change [m]	Time Driving [%]	Time Cruising [%]	Time Accelerating [%]	Time Decelerating [%]	Time Standing [%]
WLTC	23	1800	131	-	87	26	42	20	13
RDE	67	5540	123	80	80	13	33	34	20
Urban 1	1.9	600	44	18	69	11	28	30	31
Urban 2	3.1	760	55	25	67	3	31	33	33
Urban 3	3.7	1052	47	30	71	9	34	29	29
Combined 1	15	1226	115	55	78	7	37	35	22
Combined 2	31	1752	134	25	92	12	38	41	8
Combined 3	64	3582	137	161	97	15	41	41	3
Combined 4	80	3464	140	291	99	37	30	31	1
Highway	270	8246	128	680	100	72	13	16	0

3. Results and discussion

3.1. Driving cycles dynamics

Before starting with the comparison between the both powertrains, it is important to study the impact of each driving cycle in a conventional powertrain and the behavior of the ICE. For this purpose, Figure 11, Figure 12 and Figure 13 show the operating time over the total trip time in each zone of the engine map for the different cycles. Comparing the homologation cycles (Figure 11) it is possible to observe that the WLTC is more homogeneous than the RDE, with loads up to 16 bar of BMEP. On the other hand, the RDE concentrates the operation in 4 zones: two zones at 4 bar and 6 bar around 2000 rpm, one zone near 2500 rpm at 5 bar and one zone at idle operation. The last zones marked with a white square due to its higher time percentage. The RDE presents 6% higher time at idle operation than the WLTP, which could be a benefit in the hybrid operation condition due to the start stop capability.

Figure 12 shows the urban cycles are covered using the lower map zone, where the ICE generally has low efficiency and therefore a higher fuel consumption than the combined cycles is obtained. In addition, the idle operation is higher (35% of the total driving). The maximum load used for periods over 0.6% in time is around 4 bar of BMEP at 2000 rpm (10 kW) and in any case the ICE is used over 30 kW of power. In this sense, the hybrid powertrain seems to have potential to avoid the use of this part of the map and the possibility of pure electric mode in certain range of the cycle that it is zero emissions.

The combined cycles measured by the authors have similarities to the homologation ones. However, for the Combined 1 (Figure 13a), the idle time is higher than for the homologation cycles. In addition, the Combined 2 (Figure 13b) uses higher loads for more time of the total driving than the homologation ones. Lastly, the highway cycle (Figure 14) concentrates the operation over the zone of 10 bar of BMEP and 2200 rpm. The idle operation is null and the lower part of the map is not used.

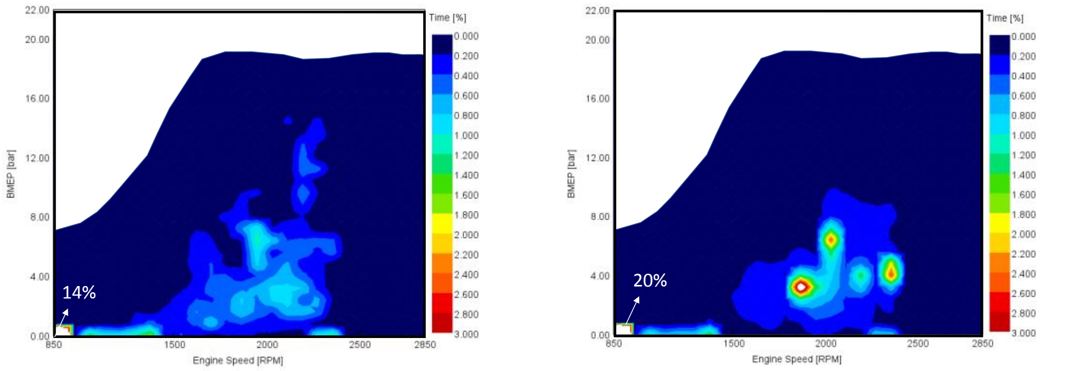

WLTC
(a)

RDE
(b)

Figure 11 – Conventional Powertrain ICE operation distribution time in percentage of the total cycle time for the homologation cycles.

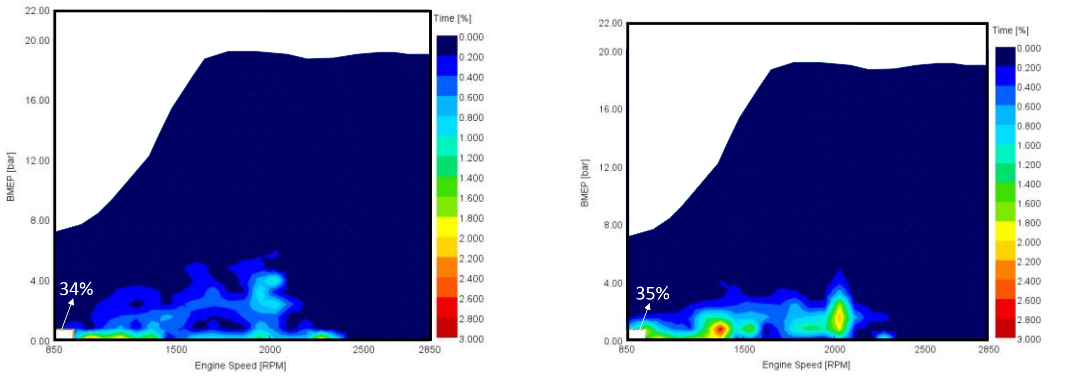

Urban 1
(a)

Urban 2
(b)

Figure 12 - Conventional Powertrain ICE operation distribution time in percentage of the total cycle time for the urban cycles.

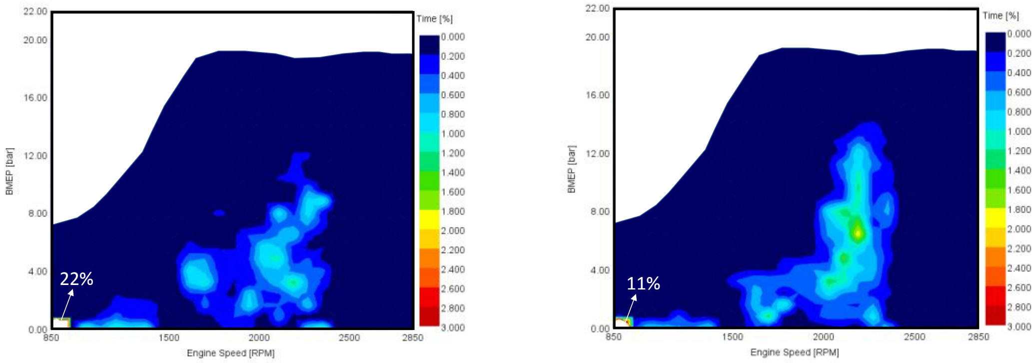

Combined 1
(a)

Combined 2
(b)

Figure 13 - Conventional Powertrain ICE operation distribution time in percentage of the total cycle time for the combined cycles.

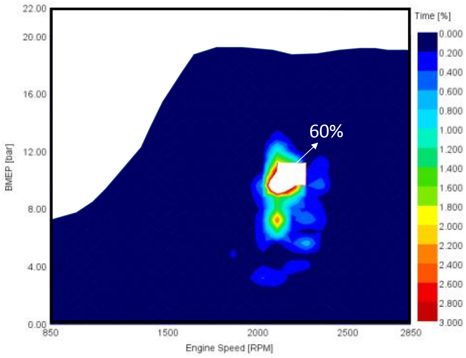

Highway

Figure 14 - Conventional Powertrain ICE operation distribution time in percentage of the total cycle time for the highway cycle.

Other parameter among the average ICE operation zones is the different acceleration of the cycles that produce instantaneous peak of power demand. Generally, these peaks are associated with higher NOx and fuel consumption. Figure 15 shows the vehicle acceleration against the vehicle speed in the homologation cycles. The higher values are found in low speed regions characteristics of the start and stop of urban areas. At high speeds, the WLTC presents a smoothed operation compared to the RDE. Figure 16 and Figure 17 show the acceleration for the real-life cycles. The urban cycle not passes 40 km/h and the acceleration distribution is closer to the low speed region of the homologation cycles. Meanwhile the combined cycles have a similar behavior than the combined reference cycles. Lastly, the highway cycle does not have practically accelerations at low speed and the distribution between accelerating and deaccelerating seems to be symmetric.

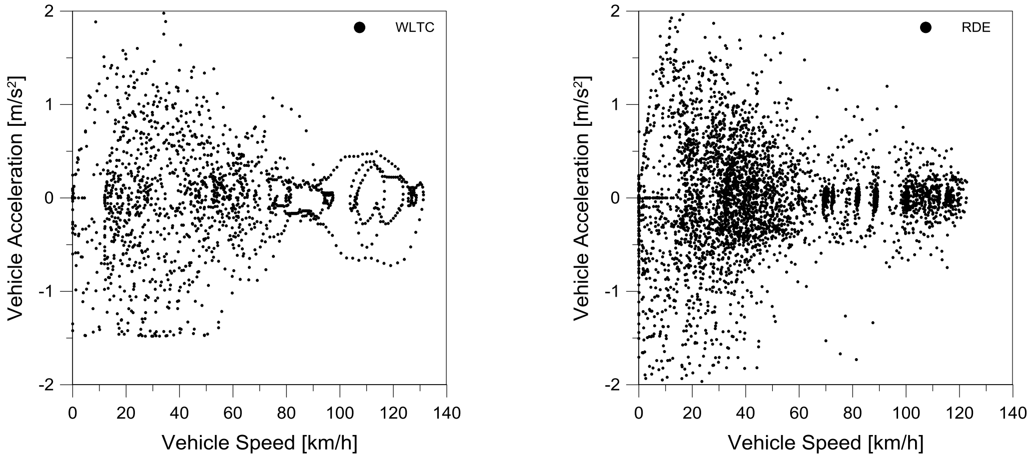

(a) (b)

Figure 15 – Acceleration distribution versus vehicle speed for the homologation cycles.

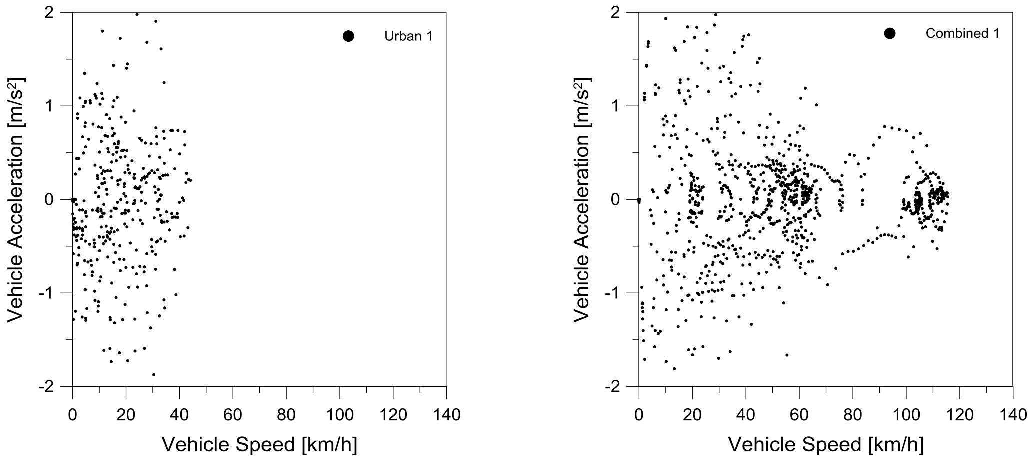

(a) (b)

Figure 16 - Acceleration distribution versus vehicle speed for a urban (a) and combined (b) real-life driving cycles.

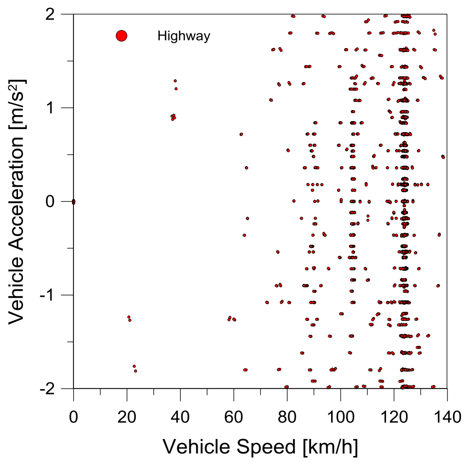

Figure 17 - Acceleration distribution versus vehicle speed for the highway real-life driving cycle.

Other crucial point in the analysis of a driving cycle is the potential energy that can be converted into electric energy by the regenerative braking mode during the reduction of vehicle speed in a driving cycle. As it is well known, in a conventional powertrain this power is absorbed by the traditional friction brakes and is released as heat. Therefore, the 100% of the energy is lost. On the other hand, in a hybrid vehicle this energy could be used by the application of a negative torque in the electric motors coupled to the transmission. The total amount of energy that can be recovered depends on the driving cycle profile, vehicle weight and electric capability of the powertrain. Therefore, previously to analyze the totally amount of energy recovered in the hybrid platform, Figure 18 shows the potential energy that is actually lost in the conventional powertrain for the different cycles. As it can be seen, the urban cycles have the highest potential to recover energy in terms of energy per kilometer.

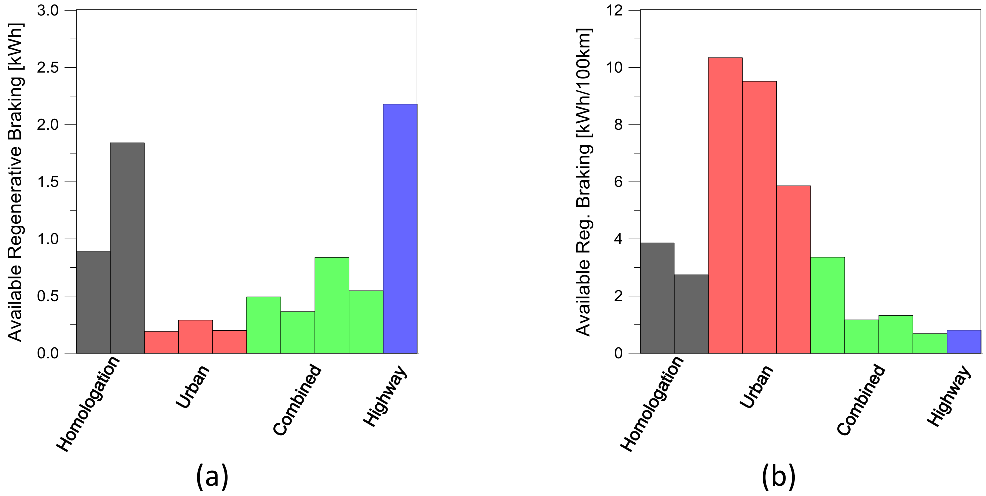

Figure 18 – Analysis of the available regenerative braking in total energy (a) and total energy for every 100km (b) of the different cycles taking the OEM vehicle.

3.2. Optimization of the hybrid powertrain for the homologation cycles

The hybrid powertrain was optimizing to meet the homologation cycle with the lowest possible fuel consumption and engine-out NOx emissions. For this purpose, a design of experiments (DoE) was created in order to test several electric components capacities and calibrate the rule based control (RBC) strategy. The DoE test matrix is shown in

Table **5**. The additional weight of each extra electric components was considered in the simulations. To take into account the extra weight of the battery package (10 kg/kWh) and the electric motor (0.7 kg/kW), representative values found in literature were used [7,35,36]. Moreover, additional 20 kg were added for the additional control units and cabling [7].

Table 5 – DoE test matrix for hybrid powertrain optimization.

Parameter	Test Range
Electric Motor Capacity	25-65 kW
Battery Package Capacity	2-15 kWh
Gear Shift Strategy	1710-2850 rpm
Maximum Speed Pure Electric Mode	25-140 km/h
Coef. Power Split	0-1.0

The different powertrain components were simulated along the WLTC. Figure 19a show the fuel consumption against the engine-out NOx emissions. It is possible to observe a trade-off between both parameters. The minimum NOx achievable is 1.1 g/km but with a high fuel consumption (5.0 lt/100km). On the other hand, the minimum fuel consumption achievable was closed to 4.4 lt/100km with 1.2 g/km of NOx. To select the optimum case, it was considered the cost to decrease the NOx engine-out to the Euro 6 emissions limit (0.08 g/km). Mera et al. [37] performed a comparison of the effectiveness of NOx reduction technologies in real-driving cycles with conventional powertrains. The best results were found for the SCR instead of lean-burn NOx trap (LNT) or the increase of exhaust gas recirculation (EGR) in the CDC. Therefore, the SCR-urea was selected for this analysis and the total urea consumption (Eq. 1) was obtained. The optimum hybrid platform is selected when the minimum total fluid consumption (fuel + urea) is achieved. As can be seen in Figure 19b, the trend is similar to Figure 19a with a shift to the right depending on the NOx emissions. The optimum case is marked with a red circle in Figure 19b.

$$Urea\ Consumption\ [{}^{g}/_{km}] = \left(NOx_{engine-out}[{}^{g}/_{km}] - 0.08\right) * 0.01 * Fuel\ consumption\ [{}^{g}/_{km}] \quad (1)$$

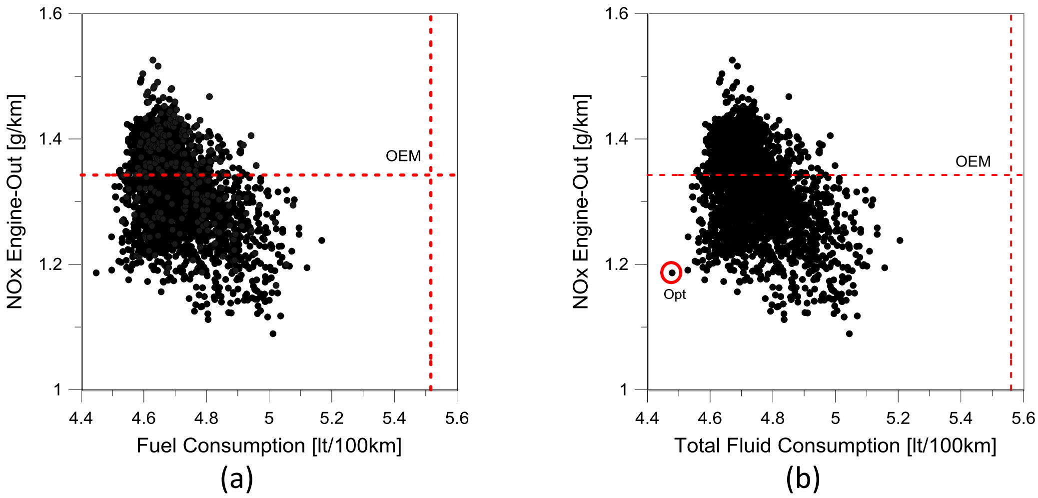

Figure 19 – Fuel consumption (a) and total fluid consumption (fuel + urea) (b) against NOx engine-out emissions in the WLTC for several hybrid powertrain configurations.

These different cases results were performed with a DoE designed to cover different hardware and control parameters as described in Table 5. One of the control parameters is the split between the ICE and the EM in the power assist mode (Coef. Power Split). This means the level of assistance that the ICE receives when the vehicle is accelerating and the battery level is over the state of charge (SOC) set point (SOC = 0.58). The variation of fuel consumption and NOx emissions with respect to the split ratio is depicted in Figure 20. The black points show the results when modifying the hardware set up while fixing the split ratio. On the other hand, the red points show the results of a study in which all the parameters have been modified at the same time. The DoE range is shown in

Table 5. Figure 20a show that it is possible to achieve a low fuel consumption (4.5 lt/100km) with all the split ratios depending on the others component selection. However, the NOx tends to increase with higher split ratios. This behavior is mainly by the effect that as more energy is used by the EM, the ICE needs to operate at higher

loads to charge the battery and therefore more NOx are emitted. On the other hand, it cannot be appreciated a notable effect in the fuel consumption because at medium (low split ratio) and high load (high split ratio) the ICE has similar efficiency.

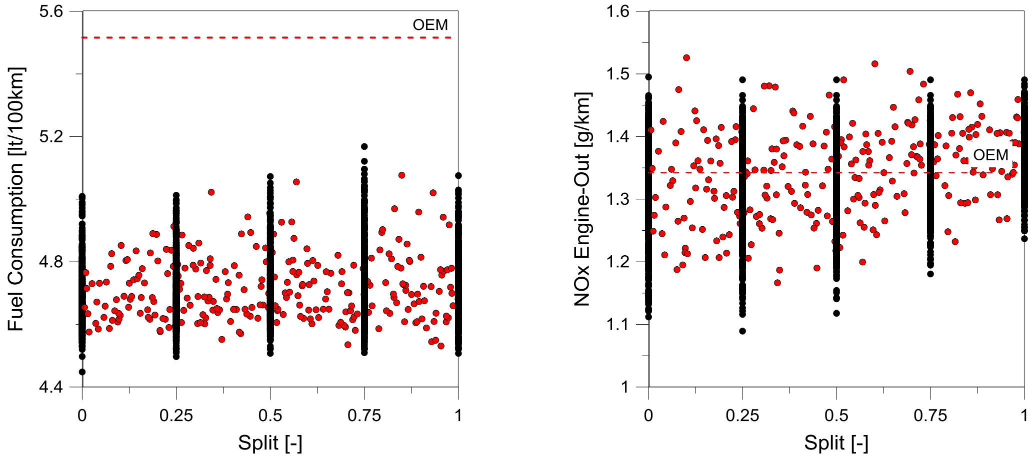

(a) (b)

Figure 20 – Split ratio between EM/ICE in power assist mode versus fuel consumption (a) and NOx engine-out emissions (b).

The gear shift, that represent the ICE rotation speed in which the gear is changed in the transmission, shows a high impact on the final results (Figure 21). The decrease of rotational speed reduces the fuel consumption because it enhances the operation at higher loads (BMEP), in which the ICE efficiency is better (Figure 4a). Figure 21a shows that the change from a high engine speed (2850 rpm) to a low engine speed (1750 rpm) reduces the fuel consumption between 4.9 to 4.6 lt/100km at the middle cases and 4.7 to 4.5 lt/100km for the minimum fuel consumption cases between both extreme engine speeds. Lower values of shift change were not studied because represent a not real driving strategy. On the other hand, the NOx has a parabolic tendency in which at low and high rotational speed have the lower emissions and at center (close to 2250 rpm) the NOx is maximum (Figure 21b). This is mainly due to the calibration map in which the medium zone of the map has the highest NOx emissions (see Figure 4b). The lowest NOx values are found with a soft shift strategy, with values 11% lower than in the central region and 4% lower than in the aggressive shift strategy.

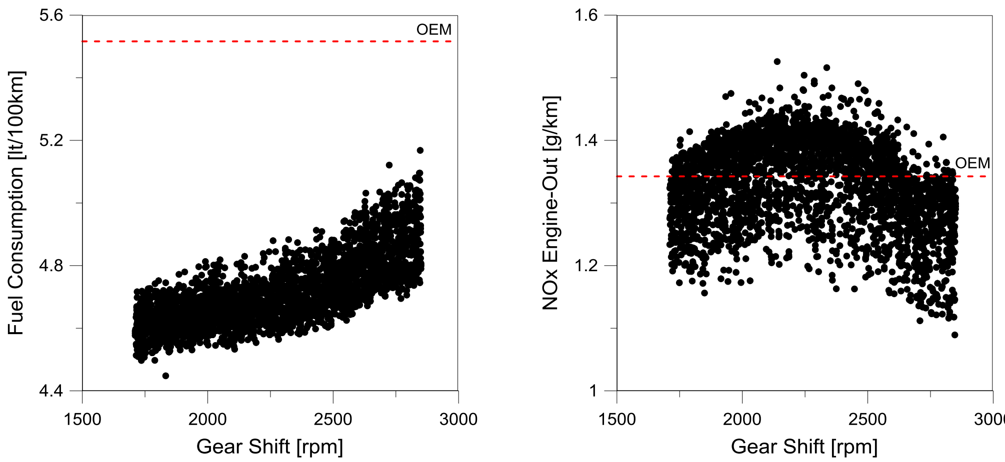

(a) (b)

Figure 21 – Fuel consumption (a) and NOx engine-out emission (b) against shift strategy for the hybrid powertrain at different set ups.

Figure 22 shows the effects of changing the pure electric top vehicle speed on fuel consumption and NOx emissions. This rule-based controller parameter set the maximum vehicle speed at which the vehicle could operate in full electric mode if the battery charge is enough charged (SOC up to 10% below of the initial charge). This parameter has a slight effect on the fuel consumption, promoting a reduction of it in of most the cases as the maximum speed is increased. The minimum fuel consumption was found at 30 km/h. On the other hand, this parameter has a great effect on the NOx emissions, with a reduction of them as the maximum speed decreases. Therefore, for this vehicle in the WLTC a low vehicle speed is preferred.

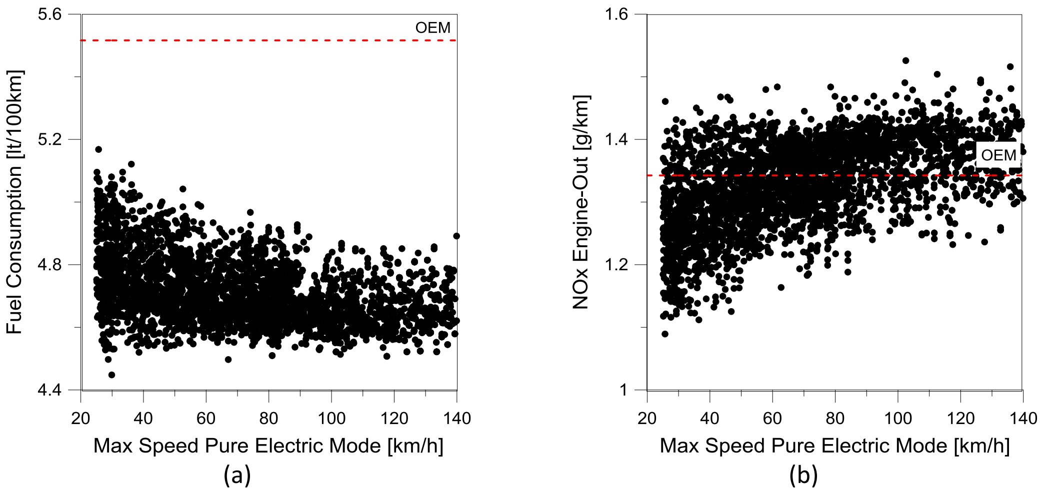

Figure 22– Fuel consumption (a) and NOx engine-out emission (b) against maximum speed to change from pure electric mode to hybrid electric mode.

The electric motor and battery capacity trends were not depicted for brevity of the manuscript. However, the influence in the final results of emissions and fuel consumption was lower than the control parameters. A summary of the optimum case is shown in Table 6 with the different electric capacities and control optimum values. As mentioned before, the optimum powertrain was considered that which leads to the lowest total fluid consumption. This means, the combination of minimum fuel and NOx emissions at engine-out. As shown in the previous graphs, the fuel consumption was below the OEM for all powertrain configurations with a maximum of 20%. On the other hand, the NOx emissions at engine-out was reduced depending on the component selection and control strategy. For this work it was supposed that the SCR-Urea system reduces the NOx to Euro 6 target (0.08 g/km) as in the OEM case. However, as the hybrid vehicle produces lower NOx than the OEM (12%), the after-treatment equipment could be relaxed in terms of capacity and effectiveness.

Table 6 – Optimum hardware and control selection to meet the WLTC with a P2 FHEV powertrain.

Parameter	Optimum Value
Electric Motor Capacity	32 kW
Battery Package Capacity	5.1 kWh
Gear Shift Strategy	1800 rpm
Maximum Speed Pure Electric Mode	30 km/h
Coef. Power Split	0

To finish the analysis of the optimum hybrid powertrain for the engine platform studied, it was performed an energy balance to detect the differences between the hybrid platform and the OEM in terms of powertrain losses. The ICE losses include the thermal efficiency and friction. The electric motor considers the electrical efficiency and friction. The battery takes into account the thermal losses for charge and discharge. The drivetrain considers the mechanical losses due to higher weights and coupling resistances of the different elements. On the other hand, in the analysis it was also considered the not recovered power due to braking. For the OEM is the total energy that the conventional friction brakes need to absorb. Lastly, the tractive losses mean the energy used to perform the driving cycle due to aerodynamic and road friction loads. At Figure 23, it is observed that the high ICE efficiency (23%) and recovery energy (37%) of the braking phase are the main improvements against the OEM. The tractive (3%) and drivetrain losses (5%) increase due to higher vehicle weight and more components including friction losses. However, it is lower than the reductions mentioned before and the total gains are of 19% in terms of energy losses reduction.

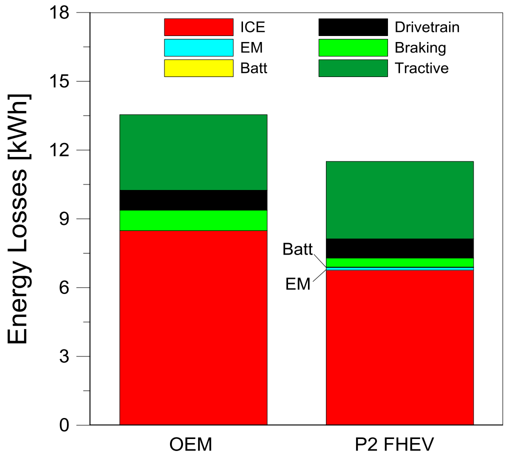

Figure 23 – Energy losses comparison between optimum P2 FHEV and OEM in the WLTC.

3.3. Performance of the optimized hybrid powertrain under real life conditions

After the optimization process of the hybrid powertrain, the focus in this section is to evaluate the effectiveness of the new vehicle set up to reduce fuel consumption and emissions. For this purpose, eight driving cycles representatives of real-life conditions were tested additionally to the WLTC and RDE that are included in the homologation legislation for passenger vehicles. It is important to note that the results obtained in this phase are without any recalibration of the thermal engine, which was design for a conventional powertrain and to meet Euro 6-d temp legislation. The authors believe that it is possible to achieve additional improvements with a dedicated recalibration of the thermal engine for the hybrid powertrain. However, it is not the objective of this work because the main idea is to evaluate the already developed Diesel ICE in real-life routes with and without an electrified powertrain.

Figure 24 shows the fuel consumption in the different cycles for the OEM and hybrid powertrain. As expected, the urban fuel consumption for a conventional powertrain is up to two times higher than in a combined cycle. The hybrid powertrain shows great potential to reduce the fuel consumption with differences up to 50% versus the OEM (red bars of Figure 24b). In combined real-life cycles, the improvement was lower than in the homologation ones, with a reduction of around 10% instead of 19% achieved in the previous section. Also, the RDE show similar fuel consumption than WLTC in both powertrains. Lastly, the highway cycle due to the selection of zero power split (optimum for WLTC) does not show gains in terms of fuel consumption. Therefore, the operation between the different powertrains for this cycle is negligible.

On the other hand, the benefits in NOx emissions reduction are not clear for hybrid powertrains (Figure 25). Looking the homologation cycles, the WLTC test shows reductions of 12% but in the RDE this benefit was low, around 6%. The urban real-life cycles show increase in the NOx emissions compared to the OEM in the same cycle. For the combined cycles the share was divided into two cycles that increase and two that decrease with respect to the OEM. However, in any case, the gains were closer to the homologation cycles (below 2%). The hybrid powertrain in the highway cycle reduces the engine-out NOx emissions around 3% compared to the OEM. Therefore, the potential to reduce NOx emissions with hybridization technology is not clear. As was mentioned before, with a dedicated recalibration of the engine control unit (ECU) for this powertrain the results could improve, especially in emissions.

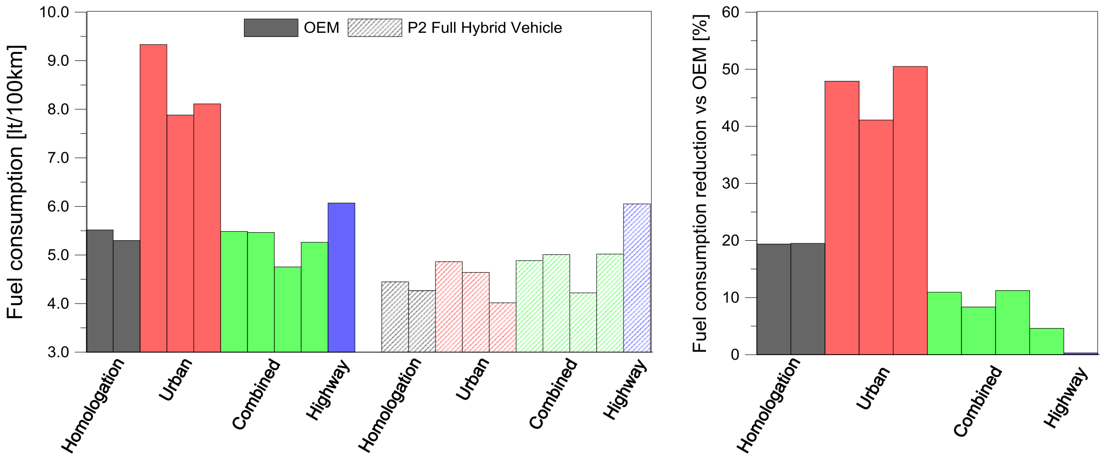

(a) (b)

Figure 24 – Fuel consumption in absolute value (a) and comparative percentage value between powertrains (b) for homologation and real-life driving cycles.

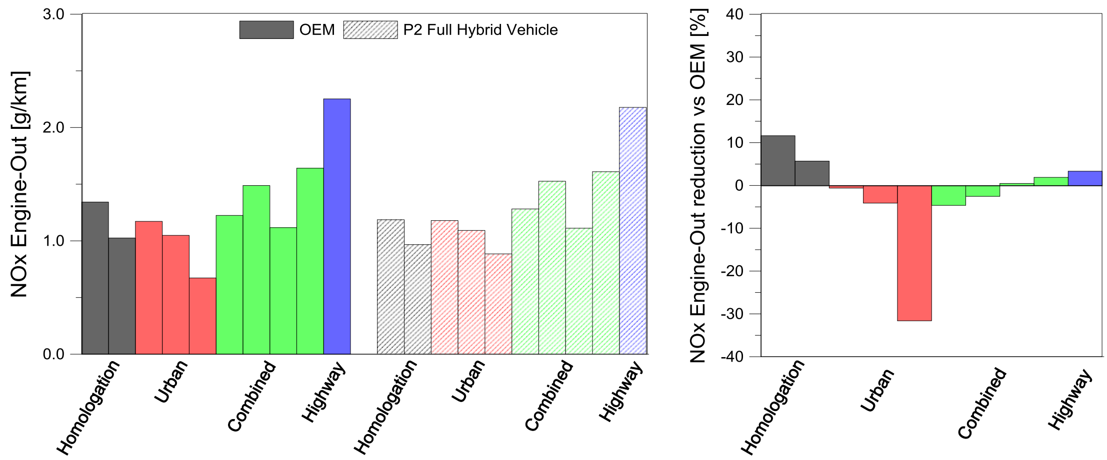

(a) (b)

Figure 25 – NOx engine-out emissions in absolute value (a) and comparative percentage value between powertrains (b) for homologation and real-life driving cycles.

To perform a deeper analysis, the urban section of the homologation cycle was compared against the three urban cycles tested previously. Figure 26a show that the benefits with real-life cycles are higher than for the homologation cycle. This can be attributed that the fact that the urban cycle used to test in the homologation cycle is not as hard as the real urban cycles tested. For the OEM in the urban 1 cycle, the fuel consumption was higher than 9.0 lt/100km, meanwhile for both homologations cycles this amount was around 6.0 lt/100km. Therefore, the potential of a hybrid powertrain combined with a Euro 6 diesel engine to reduce the fuel consumption in real urban cycles is high. The hybrid powertrain presents fuel consumption around 3.8 lt/100 km for homologation urban cycle and 4.6 lt/100 km in real urban cycles. In terms of emissions (Figure 26b), the trend in NOx was similar for homologation and real urban cycles, with an increase for almost all the cycles.

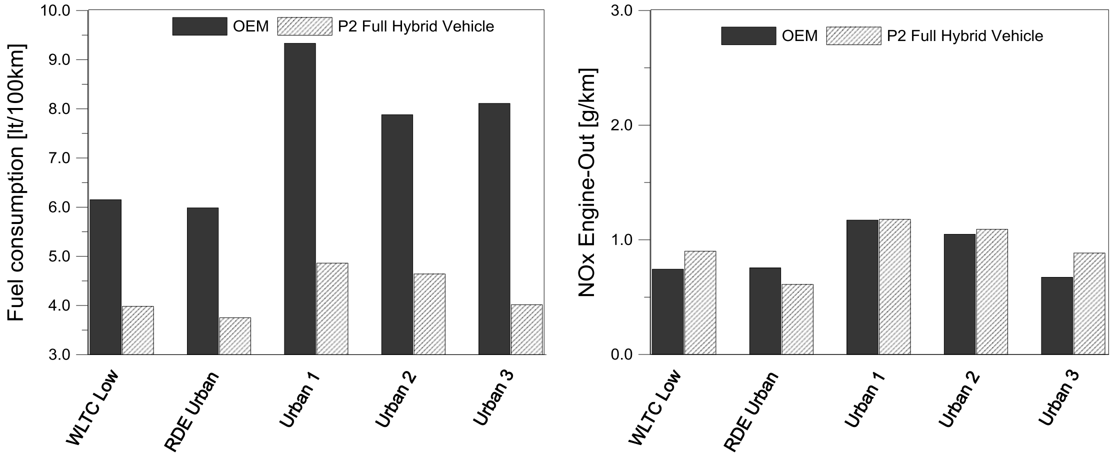

Figure 26 – Fuel consumption (a) and NOx engine-out emissions (b) for urban homologation section and urban real-life driving cycles.

It is well known that CO_2 emissions are directly related with the fuel consumption. Therefore, it is expected similar gains that was seen in Figure 24. The current legislation does not limit the fuel consumption. Instead, since 2009 the European parliament set a target to emissions of CO_2 to be meet in 2015 (130 g/km), another stricter in 2021 (95 g/km) for passenger cars. Therefore, the companies are looking for technologies that could help to achieve the desire targets. In this line, the academy tends to search for new advancements. Figure 27 shows that hybrid technology in already developed diesel engines contribute reduce the total CO_2 emissions but not achieve the 2021 target. In the homologation cycle, in which the target is considered, it is possible to pass from 143 g/km to 117 g/km (below the 2015 but above 2021 target). From the results, it is interesting to note that in urban real cycles the CO_2 emission is over 200 g/km, two times the desired target for the OEM. The hybridization strategy enables to reduce those levels up to the point to be comparable with a combined cycle. A complete summary of the engine-out emissions for the no-hybrid and hybrid powertrains in the homologation and real-life cycles are presented in Table 7. The highest improvement for the hybrid vehicle in terms of NOx and CO_2 emissions was observed in the third urban cycle, with a 31% and 47% reduction, respectively. In addition, the P2 FHEV reduces the emissions in the other two urban cycles. This result shows that the use of hybrid vehicle in cities will help to reduce local and global air pollution.

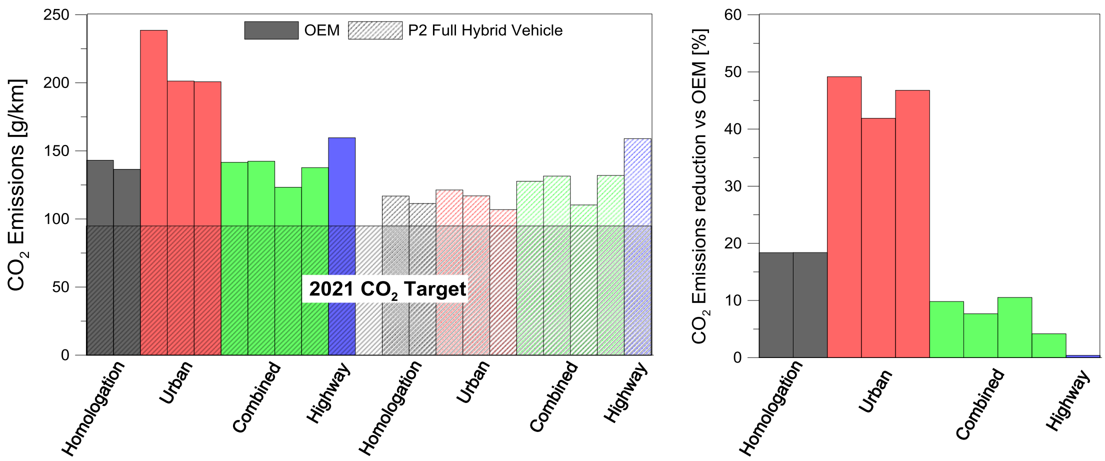

(a) (b)

Figure 27 – CO_2 engine-out emissions in absolute value (a) and comparative percentage value between powertrains (b) for homologation and real-life driving cycles.

Table 7 – Vehicle NOx and CO_2 emissions engine-out in the different homologation and real-life driving cycles.

Parameter	OEM		Hybrid		Improvement with OEM	
	NOx [g/km]	CO_2 [g/km]	NOx [g/km]	CO_2 [g/km]	NOx [%]	CO_2 [%]
WLTC	1.34	143	1.19	117	11.6	18.4
RDE	1.03	136	0.99	113	3.7	17.1
Urban 1	1.17	239	1.18	121	-0.6	49.2
Urban 2	1.05	201	1.09	117	-4.1	41.9
Urban 3	0.67	201	0.88	107	-31.6	46.8
Combined 1	1.22	142	1.28	128	-4.7	9.8
Combined 2	1.49	142	1.53	131	-2.5	7.7
Combined 3	1.12	123	1.11	110	0.5	10.5
Combined 4	1.64	138	1.61	132	1.9	4.2
Highway	2.25	160	2.18	159	3.3	0.4

These improvements are mainly explained by the increase of ICE efficiency and the regenerative braking, as was shown in the optimization section for the homologation cycle. Figure 28 shows the ICE thermal efficiency between OEM and the hybrid powertrain. The urban cycles are the most benefited with the transition from conventional to hybrid powertrains (up to 50% of improvement). On the other hand, the real combined cycles show lower benefits than the homologation.

In addition, when studying the regenerative braking use against the available regenerative energy (Figure 29a), it is possible to observe that the urban cycles show high efficiency due to the low intensity of the braking phases (see Figure 8). An opposite trend was seen for real combined cycles due to abrupt braking phases that it is not possible to use all the available energy. Also, the efficiencies are below than for the homologation cycle. The highway cycle shows an acceptable efficiency (around 60%) due to the short deceleration periods (Table 4). Figure 29b depicts the ratio between the total energy absorbed by the electric motor in the braking phases over the total tractive energy required to complete the driving cycle. For an urban cycle it represents the 40% of the used energy and for a combined cycle from 15% to 5% depends on the cycle. This enhance the potential of hybrid diesel vehicle in urban areas.

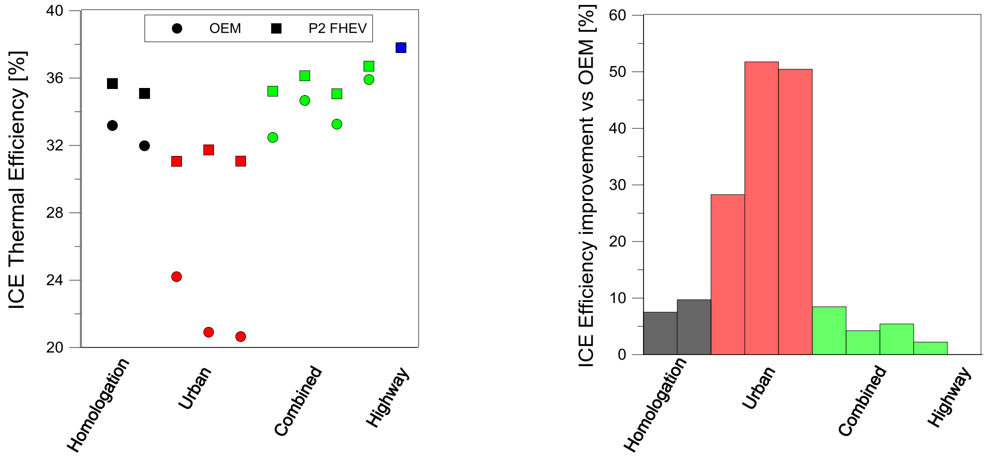

(a) (b)

Figure 28 – Internal combustion engine efficiency along the driving cycle for OEM and hybrid powertrain (a) and the improvement of hybrid with respect to the OEM (b).

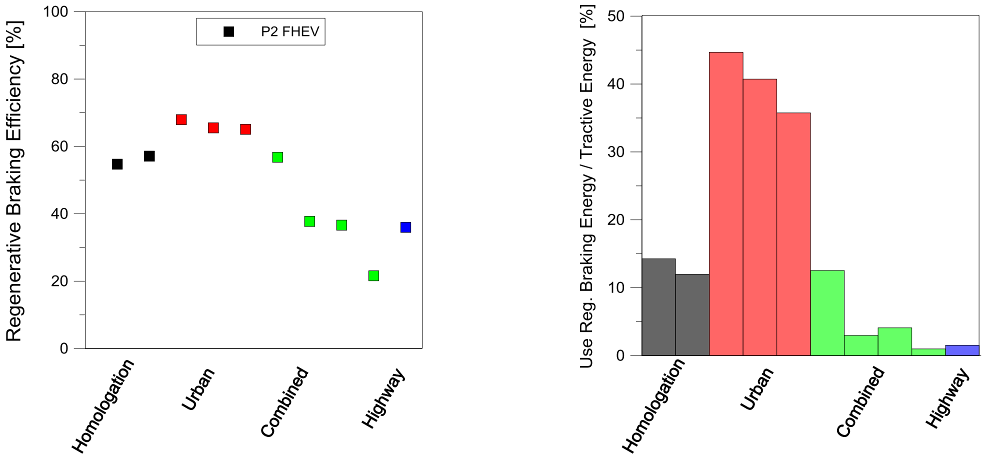

(a) (b)

Figure 29 – Regenerative braking efficiency along the driving cycle for hybrid powertrain (a) and the ratio between regenerative braking energy and the total tractive energy (b).

4. Conclusions

This work investigated the performance of two powertrain architectures representative of conventional and full hybrid commercial vehicles. The original engine calibration of a 1.6L Euro 6d-temp diesel engine was used to study the potential of the electrification of the powertrain to reduce the fuel consumption and NOx emissions. A previously developed optimization methodology was used to determine the optimum powertrain configuration under the current homologation cycle (WLTC). The numerical model was validated with experimental transient data. The behavior of the vehicle under transient conditions can be simulated with a 0D-vehicle model with sufficient precision. The differences found versus the experimental results were below 4% for fuel consumption, CO_2 and NOx emissions. After that, several real-life driving cycles were tested to see the real improvements of this technology.

From this study, it was found that:

- In the homologation cycles of the WLTP (WLTC and RDE), it is possible to save up to 20% of fuel and reduce the NOx emissions in 8% with respect to the OEM. The optimization methodology shows that the variation of shift strategy and the transition speed from pure electric to hybrid mode are the main parameters to be optimized. On the other hand, the battery capacity and electric motor size were not crucial in this process.
- The hybrid vehicle shows higher gains in urban real-life cycles than in the homologation cycle. The improvements of using a full hybrid powertrain was found around 45% in urban areas and 15% in combined cycles. The effectiveness in highway driving cycles is practically negligible.
- It was seen that the urban phase of the WLTC and RDE are softer than the cycles measured by the authors. By this reason, the OEM vehicle leads to fuel consumptions up to 9 lt/100km instead of 6 lt/100km, as measured in the homologation ones.
- In terms of engine-out NOx, all the cycles were found to produce more emission than the homologation ones. Also, for urban and some of the combined real-life cycles were higher than the OEM. This is mainly because the operation strategy, that makes the ICE to work at higher loads to re-charge the batteries and operate at higher efficiency zones.

The major reasons for the gains observed with the hybridization are the improvements of ICE efficiency along the cycle and the regenerative braking. The last one it is a source of energy that is not used in the conventional powertrain. The results show that in urban cycles the recovered energy represents around 40% of the necessary energy to perform the cycle. Lastly, the analysis of the CO_2 emissions shows a decrease of the emission levels with the hybridization of the powertrain, with gains up to 50% in urban cycles and 15% in the combined ones. The real-life highway cycle does not show greats improvements with respect to the OEM.

In spite of the improvements described, additional new technologies need to be incorporated in the vehicle to achieve the desired 2021 CO_2 targets (95g/km). A dedicated ECU recalibration work to optimize engine operation together with the electrification of the powertrain represents a potential solution. Future works of the authors will include the optimization of the engine map zone to reduce fuel consumption and NOx emissions to achieve the desired targets.

Acknowledgments

The authors acknowledge FEDER and Spanish Ministerio de Economía y Competitividad for partially supporting this research through TRANCO project (TRA2017-87694-R). The authors also acknowledge the Universitat Politècnica de València for partially supporting this research through Convocatoria de ayudas a Primeros Proyectos de Investigación (PAID-06-18).

References

[1] Luján JM, Bermúdez V, Dolz V, Monsalve-Serrano J. An assessment of the real-world driving gaseous emissions from a Euro 6 light-duty diesel vehicle using a portable emissions measurement system (PEMS). Atmos Environ 2018;174:112–21. doi:10.1016/j.atmosenv.2017.11.056.

[2] García A, Monsalve-Serrano J, Villalta D, Lago Sari R. Performance of a conventional diesel aftertreatment system used in a medium-duty multi-cylinder dual-mode dual-fuel engine. Energy Convers Manag 2019;184:327–37. doi:10.1016/j.enconman.2019.01.069.

[3] Williams M, Minjares R. Report: A technical summary of Euro 6/VI vehicle emission standards. The International Council on Clean Transportation. 2016.

[4] Council GS of the. Proposal for a Regulation of the European Parliament and of the Council setting emission performance standards for new passenger cars and for new light commercial vehicles as part of the Union's integrated approach to reduce CO2 emissions from light-duty. Brussels: 2019.

[5] Thiyagarajan S, Varuvel EG, Martin LJ, Beddhannan N. Mitigation of carbon footprints through a blend of biofuels and oxygenates, combined with post-combustion capture system in a single cylinder CI engine. Renew Energy 2019;130:1067–81. doi:10.1016/j.renene.2018.07.010.

[6] Huang Y, Wang H, Khajepour A, Li B, Ji J, Zhao K, et al. A review of power management strategies and component sizing methods for hybrid vehicles. Renew Sustain Energy Rev 2018;96:132–44. doi:10.1016/j.rser.2018.07.020.

[7] Sarlioglu B, Morris CT, Han D, Li S. Benchmarking of electric and hybrid vehicle electric machines, power electronics, and batteries. 2015 Intl Aegean Conf. Electr. Mach. Power Electron. (ACEMP), 2015 Intl Conf. Optim. Electr. Electron. Equip. 2015 Intl Symp. Adv. Electromechanical Motion Syst., IEEE; 2015, p. 519–26. doi:10.1109/OPTIM.2015.7426993.

[8] Negoro AB, Purwadi A. Performance Analysis on Power Train Drive System of the 2012 Toyota Camry Hybrid. Procedia Technol 2013;11:1054–64. doi:10.1016/j.protcy.2013.12.294.

[9] Qiao Q, Zhao F, Liu Z, Jiang S, Hao H. Comparative Study on Life Cycle CO2 Emissions from the Production of Electric and Conventional Vehicles in China. Energy Procedia 2017;105:3584–95. doi:10.1016/j.egypro.2017.03.827.

[10] Rupp M, Handschuh N, Rieke C, Kuperjans I. Contribution of country-specific electricity mix and charging time to environmental impact of battery electric vehicles: A case study of electric buses in Germany. Appl Energy 2019;237:618–34. doi:10.1016/j.apenergy.2019.01.059.

[11] Liu H, Brown T, Andresen GB, Schlachtberger DP, Greiner M. The role of hydro power, storage and transmission in the decarbonization of the Chinese power system. Appl Energy 2019;239:1308–21. doi:10.1016/j.apenergy.2019.02.009.

[12] Chan CC. The state of the art of electric, hybrid, and fuel cell vehicles. Proc IEEE

2007;95:704–18. doi:10.1109/JPROC.2007.892489.

[13] Gupta AK, Kartik V, Ramanarayanan CP. Experimental Study on Performance of a Parallel Diesel Hybrid Vehicle Retrofitted with a Single Planetary Gear Train as an Add-On Transmission 2016. doi:10.4271/2016-28-0154.

[14] Babu A, Ashok S. Energy and fuel efficient parallel mild hybrids for urban roads. Energy Convers Manag 2016;121:305–20. doi:10.1016/j.enconman.2016.05.047.

[15] Roberts PJ, Mumby R, Mason A, Redford-Knight L, Kaur P. RDE Plus - The Development of a Road, Rig and Engine-in-the-Loop Test Methodology for Real Driving Emissions Compliance. SAE Int 2019:1–12. doi:10.4271/2019-01-0756.Abstract.

[16] Achour H, Carton JG, Olabi AG. Estimating vehicle emissions from road transport, case study: Dublin City. Appl Energy 2011;88:1957–64. doi:10.1016/j.apenergy.2010.12.032.

[17] Tutuianu M, Bonnel P, Ciuffo B, Haniu T, Ichikawa N, Marotta A, et al. Development of the World-wide harmonized Light duty Test Cycle (WLTC) and a possible pathway for its introduction in the European legislation. Transp Res Part D Transp Environ 2015;40:61–75. doi:10.1016/j.trd.2015.07.011.

[18] Varella R, Giechaskiel B, Sousa L, Duarte G. Comparison of Portable Emissions Measurement Systems (PEMS) with Laboratory Grade Equipment. Appl Sci 2018;8:1633. doi:10.3390/app8091633.

[19] Salim WSIW, Mahdi AAM, Ismail MI, Abas MA, Martinez-Botas RF, Rajoo S. Benefits of spark-ignition engine fuel-saving technologies under transient part load operations. J Mech Eng Sci ISSN 2017;11:2289–4659. doi:10.15282/jmes.11.4.2017.6.0272.

[20] Demuynck J, Favre C, Bosteels D, Hamje H, Andersson J. Real-World Emissions Measurements of a Gasoline Direct Injection Vehicle without and with a Gasoline Particulate Filter. WCX^{TM} 17 SAE World Congr. Exp., SAE International; 2017. doi:https://doi.org/10.4271/2017-01-0985.

[21] Puškár M, Jahnátek A, Kádárová J, Šoltésová M, Kovanič Ľ, Krivosudská J. Environmental study focused on the suitability of vehicle certifications using the new European driving cycle (NEDC) with regard to the affair “dieselgate” and the risks of NO x emissions in urban destinations. Air Qual Atmos Heal 2019;12:251–7. doi:10.1007/s11869-018-0646-5.

[22] Mera Z, Fonseca N, López JM, Casanova J. Analysis of the high instantaneous NO x emissions from Euro 6 diesel passenger cars under real driving conditions. Appl Energy 2019;242:1074–89. doi:10.1016/j.apenergy.2019.03.120.

[23] Benajes J, García A, Monsalve-Serrano J, Boronat V. Dual-Fuel Combustion for Future Clean and Efficient Compression Ignition Engines. Appl Sci 2016;7:36. doi:10.3390/app7010036.

[24] García A, Monsalve-Serrano J, Rückert Roso V, Santos Martins ME. Evaluating the emissions and performance of two dual-mode RCCI combustion strategies

under the World Harmonized Vehicle Cycle (WHVC). Energy Convers Manag 2017;149:263–74. doi:10.1016/j.enconman.2017.07.034.

[25] Solouk A, Shakiba-Herfeh M, Arora J, Shahbakhti M. Fuel consumption assessment of an electrified powertrain with a multi-mode high-efficiency engine in various levels of hybridization. Energy Convers Manag 2018;155:100–15. doi:10.1016/j.enconman.2017.10.073.

[26] Huo Y, Yan F, Feng D. A hybrid electric vehicle energy optimization strategy by using fueling control in diesel engines. Proc Inst Mech Eng Part D J Automob Eng 2019;233:517–30. doi:10.1177/0954407017747372.

[27] Mamikoglu S, Andric J, Dahlander P. Impact of Conventional and Electrified Powertrains on Fuel Economy in Various Driving Cycles. SAE Tech. Pap. Ser., vol. 1, 2017. doi:10.4271/2017-01-0903.

[28] Council on Clean Transportation I. European Vehicle Market Statistics 2017/2018 2017:63.

[29] Morra E, Spessa E, Ciaravino C, Vassallo A. Analysis of Energy-Efficient Management of a Light-Duty Parallel-Hybrid Diesel Powertrain with a Belt Alternator Starter. SAE Int J Altern Powertrains 2012;1:2012-01–1008. doi:10.4271/2011-24-0080.

[30] Fahrzeug- AK, Vassallo A, Cipolla G, Mallamo F, Paladini V, Powertrain GM, et al. Transient Correction of Diesel Engine Steady- State Emissions and Fuel Consumption Maps for Vehicle Performance Simulation. Aachener Kolloquium Fahrzeug- und Mot., 2007.

[31] Benajes J, García A, Monsalve-Serrano J, Martínez-Boggio S. Optimization of the parallel and mild hybrid vehicle platforms operating under conventional and advanced combustion modes. Energy Convers Manag 2019;190:73–90. doi:10.1016/j.enconman.2019.04.010.

[32] Morra E, Spessa E, Ciaravino C, Vassallo A. Analysis of Various Operating Strategies for a Parallel-Hybrid Diesel Powertrain with a Belt Alternator Starter. SAE Int J Altern Powertrains 2012;1:2012-01–1008. doi:10.4271/2012-01-1008.

[33] United Nations. GTR 15 - Global Registry Worldwide harmonized Light vehicles Test Procedure. Glob Regist 2014.

[34] Commission Regulation (EU) 2016/427 of 10 March 2016 amending Regulation (EC) No 692/2008 as regards emissions from light passenger and commercial vehicles (Euro 6). Off. J. Eur. Union L82, 1–98 European Commission. 2016.

[35] Nikolian A, Firouz Y, Gopalakrishnan R, Timmermans JM, Omar N, van den Bossche P, et al. Lithium ion batteries-development of advanced electrical equivalent circuit models for nickel manganese cobalt lithium-ion. Energies 2016;9:360. doi:10.3390/en9050360.

[36] Gan S, Chrenko D, Kéromnès A, Le Moyne L. Development of a Multi-Architecture and Multi-Application Hybrid Vehicle Design and Management Tool. Energies 2018;11:3185. doi:10.3390/en11113185.

[37] Mera Z, Fonseca N, López J-M, Casanova J. Analysis of the high instantaneous NOx emissions from Euro 6 diesel passenger cars under real driving conditions. Appl Energy 2019;242:1074–89. doi:10.1016/j.apenergy.2019.03.120.

Abbreviations

BMEP	Brake mean effective pressure	LRF	Low Reactivity Fuel
BMS	Battery management system	LTC	Low Temperature Combustion
$BSCO_2$	Brake specific CO_2 emissions	MHEV	Mild hybrid electric vehicle
BSFC	Brake specific fuel consumption	MPRR	Maximum Pressure Rise Rate
BSNOx	Brake specific NOx emissions	NEDC	New European Driving Cycle
CDC	Conventional diesel combustion	NOx	Nitrogen Oxides
CI	Compression Ignition	NOxEU6	Nitrogen oxide limit for Euro VI legislation
CO	Carbon Monoxide	OEM	Oroiginal equipment manufacturer
DI	Direct Injection	P0	Belt alternator starte hybrid powertrain
DOC	Diesel Oxidation Catalysts	P2	Parallel hybrid electric vehicle
DoE	Design of Experiments	P2-FHEV	Parallel full hybrid electric vehicle
DPF	Diesel Particulate Filter	PEMS	Portable measurement system
ECU	Engine control unit	PFI	Port fuel injection
EGR	Exhaust Gas Recirculation	PHEV	Plug in electric vehicle
EM	Electric motor	RBC	Rule base control
EMS	Energy managment system	RCCI	Reactivity Controlled Compression Ignition
EU	European Union	RDE	Real driving emission test
Evs	Electric vehicles	rpm	Revolution per minute
FHEV	Full hybrid vehicle	SCE	Single Cylinder Engine
HC	Unburned Hydrocarbons	SCR	Selective Catalytic Reduction
HCCI	Homogeneous Charge Compression Ignition	SI	Spark Ignition
HEV	Hybrid electric vehicle	SOC	State of the charge of the battery
HRF	High Reactivity Fuel	VGT	Variable geometry turbine
ICE	Internal combustion engine	WLTC	Worldwide Harmonized Light Vehicles Cycle
LI-Ion	Litium Ion batteries	WLTP	Worldwide Harmonized Light Test Procedure
LNT	Lean NOx tramp	WTW	Well to wheel